Divya Chalise
Mechanical and Aerospace Engineering Department, University of Texas at Arlington, Arlington, TX 76019

Krishna Shah
Mechanical and Aerospace Engineering Department, University of Texas at Arlington, Arlington, TX 76019

Ravi Prasher
Energy Storage and Distributed Resources Division, Lawrence Berkeley National Laboratory, Berkeley, CA 94720
Department of Mechanical Engineering, University of California, Berkeley, Berkeley, CA 94720

Ankur Jain[1]
Mechanical and Aerospace Engineering Department, University of Texas at Arlington, 500 W First Street, Room 211, Arlington, TX 76019
e-mail: jaina@uta.edu

Conjugate Heat Transfer Analysis of Thermal Management of a Li-Ion Battery Pack

Thermal management of Li-ion battery packs is a critical technological challenge that directly impacts safety and performance. Removal of heat generated in individual Li-ion cells into the ambient is a considerably complicated problem involving multiple heat transfer modes. This paper develops an iterative analytical technique to model conjugate heat transfer in coolant-based thermal management of a Li-ion battery pack. Solutions for the governing energy conservation equations for thermal conduction and convection are derived and coupled with each other in an iterative fashion to determine the final temperature distribution. The analytical model is used to investigate the dependence of the temperature field on various geometrical and material parameters. This work shows that the coolant flowrate required for effective cooling can be reduced significantly by improving the thermal conductivity of individual Li-ion cells. Further, this work helps understand key thermal–electrochemical trade-offs in the design of thermal management for Li-ion battery packs, such as the trade-off between temperature rise and energy storage density in the battery pack. [DOI: 10.1115/1.4038258]

Keywords: Li-ion battery pack, thermal analysis, conjugate heat transfer, battery safety

1 Introduction

Effective removal of heat from Li-ion cells and battery packs is a critical technological challenge for improving the performance, safety, and reliability of electrochemical energy conversion and storage systems [1–3]. Several engineering applications such as electric vehicles, stationary power storage systems, etc., involve large battery packs containing multiple Li-ion cells capable of individually storing and converting energy. Heat generated within each Li-ion cell during charge/discharge must be eventually rejected to the ambient. This process must occur with minimal thermal resistance in order to minimize the temperature rise in each Li-ion cell [4,5]. The path of heat transfer from within each cell to the ambient is somewhat involved [6]. During this process, heat must conduct through materials and interfaces within each cell, then into any surrounding materials, followed by convection into the coolant fluid, which carries the heat away from the battery pack and eventually rejects it to the ambient [7]. Pack-level thermal management plays a key role in overall thermal performance of a battery pack [3]. However, effective, active thermal management may require components such as coolant channels, pump, etc., that do not contribute to energy storage and may even consume energy. While the thermal management system must ensure effective heat removal, the nonelectrochemical components in the pack must be minimized in order to increase the energy storage density and reduce overall weight. The development of accurate thermal modeling tools is critical for reconciling such design trade-offs and designing battery packs that maximize energy storage density while limiting the temperature rise and temperature gradient within the pack.

Significant past work is available on both experimental measurements and modeling of pack-level thermal management of Li-ion battery packs. A variety of thermal management approaches, including heat pipe-based cooling, convective cooling, etc., has been investigated. Both air- and liquid-based thermal management has been demonstrated experimentally for Li-ion battery packs [8–14]. Water is the most commonly investigated liquid coolant. The use of liquid cooling plates has been investigated. Various cell arrangements in a Li-ion battery pack along with different cooling duct configurations have been experimentally evaluated for air cooling [8–11]. Similarly, liquid-based cooling using cooling plates with microchannels of different configurations placed between batteries has been reported [12–14]. Some work also exists on the use of low boiling point dielectric liquids for thermal management [15,16]. Heat pipes and phase change materials have been inserted in the battery pack in order to absorb heat generated in the cell and minimize temperature rise [17–30]. A number of papers have utilized finite element simulations to numerically characterize the performance of such thermal management systems. Air [10,11,21–36], liquid [12–14,37–40], heat pipe, [36] and phase change materials [27,41,42] based thermal management approaches have been evaluated by pack-level simulations. The modeling of different cooling configurations [31–33], cell arrangements [10,11,34], and flow duct design [32] for enhanced natural convection has been carried out. Similarly, liquid cooling-based thermal management strategies have been analyzed through simulations. This includes design of liquid cooling plate [12,13,38–40], thermal optimization [38–40], and evaluation of different cooling strategies [14,37]. Numerical simulations on using phase change materials [41,42] and heat pipes [36] for pack-level thermal management have also been reported. While significant temperature reduction has been shown in these various simulations-based analysis, the impact of these cooling strategies in terms of reduced pack level energy storage density has often been neglected.

While finite element simulations offer convenience in determining temperature rise in a specific geometry, such simulations can often be time-consuming to setup and execute. More importantly, there are often challenges in interfacing such simulations with the battery management system, which is a critical need for thermally driven battery performance management. An alternative to finite element simulations is analytical derivation of the solution of

[1]Corresponding author.

Manuscript received May 15, 2017; final manuscript received September 27, 2017; published online November 28, 2017. Assoc. Editor: George Nelson.

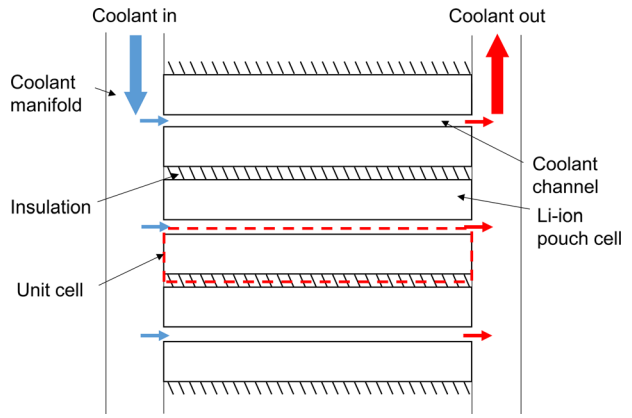

Fig. 1 Schematic of the geometry for air/liquid cooling of a prismatic Li-ion battery pack, also showing the fundamental thermal unit cell within dashed lines

energy conservation equations that govern the temperature field in the system. While mathematically more challenging, such analytical modeling approach results in closed form solutions of the temperature distribution that provide useful physical insights into the heat transfer process that is not possible through simulations. For example, once a closed-form solution for the temperature field is available, the effect of various geometrical parameters and thermophysical properties can be rapidly evaluated. Closed-form solutions are also easier to interface with other computational tools, such as electrochemistry models, for multiphysics co-optimization during the design process, or during real-time operation. However, analytical approaches are mathematically more challenging than finite element simulations and geometrical approximations may be needed. Air/liquid cooling of a Li-ion battery pack is a conjugate heat transfer problem involving both thermal conduction in the solid battery and thermal convection to the coolant flow. The modeling of such conjugate problems is not straightforward. While conjugate heat transfer models have been developed for simple conditions, there is relatively limited work available on analyzing conjugate heat transfer in more complicated situations such as those that may be encountered in realistic battery packs. In the recent past, a general, iterative method has been developed for analytical modeling of conjugate heat transfer in solid–fluid domains [43] such as the cooling of Li-ion cells using a coolant flow. This method is based on solving the thermal conduction and convection problems separately. Utilizing temperature and heat flux matching at the solid–liquid interface, the output of one problem is utilized to solve the other in an iterative fashion. This approach has been shown to work well for a broad class of conjugate problems involving external and internal flow [43].

This paper presents conjugate heat transfer analysis for the cooling of a Li-ion cell battery pack. An iterative analytical approach is used to investigate fundamental processes that govern temperature rise in a Li-ion battery pack. The dependence of the temperature field on various geometrical and material parameters is investigated. The analytical model helps understand thermal management of Li-ion battery packs, and assists in understanding and quantifying various thermal–electrochemical tradeoffs that arise in the design of a Li-ion battery pack. These results may contribute toward improved thermal design and run-time thermal performance of Li-ion battery packs.

2 Theoretical Model

The problem of cooling of a Li-ion cell in a battery pack with a fluid flow such as air or water is shown schematically in Fig. 1, where multiple cells in a battery pack are to be cooled. Figure 1 also identifies the unit cell that repeats itself in the battery pack. The temperature field within this unit cell is to be determined as a function of geometry, operating parameters of the cell, such as C-rate, thermal properties, as well as the parameters and properties related to the coolant fluid. Specific quantities of interest may include the peak temperature rise in the cell, temperature gradient within the cell, pressure drop in the coolant fluid, etc. This is a conjugate heat transfer problem as it involves heat transfer through conduction within the solid cell and convective heat transfer to the cooling fluid. While problems involving conduction or convection only are easier to address by directly solving the underlying energy conservation equation in the solid or liquid, a conjugate problem is considerably more complicated due to the interaction between the solid and fluid. In this case, an iterative analytical technique is utilized for solving the conjugate problem [43]. The technique utilizes continuity of temperature and energy conservation at the solid–liquid interface to iteratively solve the conduction and convection problems separately [43]. The solution of each problem provides a boundary condition for the other problem. The iterative solution process continues to until sufficient accuracy is reached.

In this specific case, Fig. 2(*a*) shows the solid domain of the conjugate problem in the thermal unit cell. The steady-state temperature rise in the solid domain, $T_s(x, y)$ satisfies the following energy conservation equation:

$$k_{x,s}\frac{\partial^2 T_s}{\partial x^2} + k_{y,s}\frac{\partial^2 T_s}{\partial y^2} + Q''' = 0 \tag{1}$$

and the following boundary conditions:

$$k_{x,s}\frac{\partial T_s}{\partial x} = hT_s \quad \text{at } x = 0 \tag{2}$$

$$-k_{x,s}\frac{\partial T_s}{\partial x} = hT_s \quad \text{at } x = L \tag{3}$$

$$\frac{\partial T_s}{\partial y} = 0 \quad \text{at } y = 0 \tag{4}$$

$$-k_{y,s}\frac{\partial T_s}{\partial y} = q_0''(x) \quad \text{at } y = H \tag{5}$$

Q''' is the volumetric heat generation due to charge/discharge, $k_{x,s}$ and $k_{y,s}$ are the orthotropic thermal conductivities and h is the

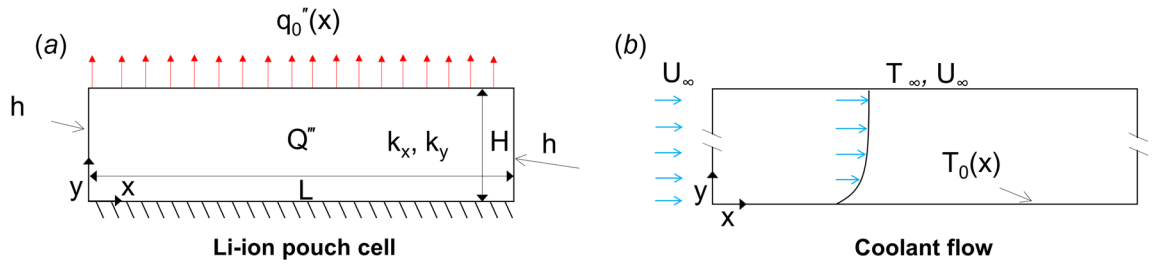

Fig. 2 Definitions of the individual (*a*) solid and (*b*) fluid problems that make up the conjugate heat transfer problem

convective heat transfer coefficient on the edges of the cell. Note that $q_0''(x)$ is the heat flux at the solid–fluid interface and is not known in advance. The fluid domain of the thermal unit cell comprises the coolant flow shown in Fig. 2(*b*). Temperature rise distribution in the fluid domain is governed by

$$\alpha_f \frac{\partial^2 T_f}{\partial y^2} = u\frac{\partial T_f}{\partial x} + v\frac{\partial T_f}{\partial y} \tag{6}$$

where viscous dissipation is neglected.

Finally, at the solid–fluid interface

$$T_f = T_s \tag{7}$$

and

$$k_{y,s}\frac{\partial T_s}{\partial y} = k_f \frac{\partial T_f}{\partial y} \tag{8}$$

for temperature continuity and conservation of energy, respectively.

The conjugate problem described in Eqs. (1)–(8) is solved in an iterative approach. For the fluid domain, Eq. (6) is solved based on a flow over a flat plate problem with an assumed temperature distribution $T_0(x)$ at the interface

$$T_f = T_0(x) \quad \text{at } y = 0 \tag{9}$$

A solution for this problem has been derived by integrating the effect of infinitesimal sections of the flat plate with given temperature rise of the interface [44]. The final solution for the temperature distribution in the coolant fluid is given by [44]

$$T_f(x,y) = \int_0^x [1-\theta(\xi,x,y)]\frac{dT_0}{d\xi}d\xi + \sum_{i=1}^{k}[1-\theta(\xi_i,x,y)]T_0(i) \tag{10}$$

where the function $\theta\,(\xi, x, y)$ is given by

$$\theta(\xi,x,y) = \frac{0.331\,\mathrm{Pr}^{1/3}\,\mathrm{Re}_x^{1/2} y}{x\left[1-\left(\frac{\xi}{x}\right)^{3/4}\right]^{1/3}} - \frac{0.005405\,\mathrm{Pr}\,\mathrm{Re}_x^{3/2} y^3}{x^3\left[1-\left(\frac{\xi}{x}\right)^{3/4}\right]} \tag{11}$$

In Eq. (10), the integration and the summation accounts for the continuous variation and step changes in T_0, respectively. This equation assumes that the dimensions of the coolant channel cross section are larger than the expected maximum boundary layer size.

The interface heat flux can be computed from Eqs. (10) and (11) as follows [44]:

$$\begin{aligned} q_0''(x) &= -k_y\frac{\partial T_f}{\partial y}\bigg|_{y=0} \\ &= k_y\left[\int_0^x \frac{\partial\theta}{\partial y}(\xi,x,0)\frac{dT_0}{d\xi}d\xi + \sum_{i=1}^{k}\frac{\partial\theta}{\partial y}(\xi_i,x,0)T_0(i)\right] \end{aligned} \tag{12}$$

This heat flux is used to solve the solid problem defined by Eqs. (1)–(5) by first splitting the problem into two problems followed by the use of the separation of variables technique [45].

Temperature rise in the solid domain, $T_s(x, y)$ can be determined by splitting into two components [45]

$$T_s(x,y) = s(x) + w(x,y) \tag{13}$$

The two components of the temperature distribution are given by

$$s(x) = \frac{Q'''}{2k_{x,s}}\left[x(L-x) + \frac{L^2}{Bi_L}\right] \tag{14}$$

and

$$\begin{aligned} w(x,y) = \sum_{n=1}^{\infty} C_n \mathrm{Cosh}\left(\sqrt{\frac{k_{x,s}}{k_{y,s}}}\mu_n y\right) \\ \cdot\left[\mu_n L\mathrm{Cos}(\mu_n x) + Bi_L \mathrm{Sin}(\mu_n x)\right] \end{aligned} \tag{15}$$

The coefficients C_n in Eq. (15) are given by

$$C_n = \frac{-\frac{1}{L}\int_0^L q_0''(x)\cdot\left[\mu_n L\mathrm{Cos}(\mu_n x) + Bi_L\mathrm{Sin}(\mu_n x)\right]dx}{\frac{1}{2}\cdot\left[\left(\mu_n L\right)^2 + Bi_L^2\right)\left(1+\frac{Bi_L}{\left(\mu_n L\right)^2 + Bi_L^2}\right) + Bi_L\Bigg]\cdot\left[\mu_n\sqrt{\frac{k_{x,s}}{k_{y,s}}}k_y\mathrm{Sinh}\left(\sqrt{\frac{k_{x,s}}{k_{y,s}}}\mu_n H\right)\right]} \tag{16}$$

The eigenvalues μ_n are obtained from roots of the transcendental equation

$$\mathrm{Tan}(\mu L) = \frac{2Bi_L\cdot(\mu L)}{(\mu L)^2 - Bi_L^2} \tag{17}$$

where $Bi_L = hL/k_{x,s}$.

In the solid problem, the interface temperature distribution $T_0(x)$ is calculated by substituting $y = H$ in Eq. (3), which is used to solve the fluid problem again. The iterative process is continued until convergence is reached. In practice, the interface temperature distribution is updated to a blend of the newly calculated and older distributions. If $T_{0,\mathrm{old}}(x)$ represents the interface temperature at the present iteration, the new the interface temperature distribution is obtained by

$$T_{0,\mathrm{new}}(x) = \beta T_s(x, y = H) + (1-\beta)T_{0,\mathrm{old}}(x) \tag{18}$$

The blend factor β is kept low enough in order to prevent divergence in the temperature distribution with increasing number of iterations.

In summary, the iterative approach utilized here starts with an assumed temperature profile at the solid–fluid interface, solves the fluid problem to provide a heat flux input that enables the solution of the solid problem [43]. The solution for the solid problem is then used to determine a new temperature profile at the solid–fluid interface. This process is repeated iteratively until convergence [43]. Figure 3 shows a schematic of this iterative procedure.

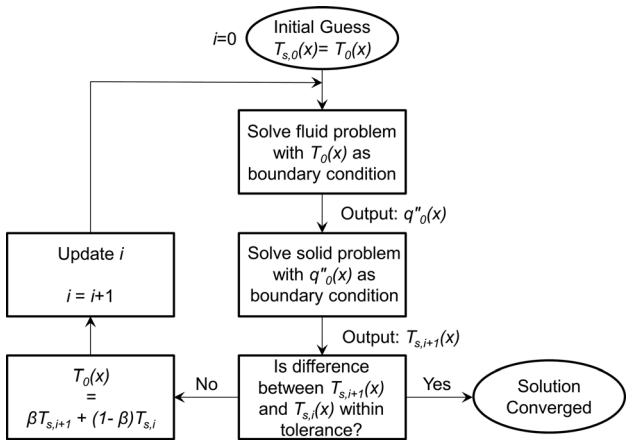

Fig. 3 Schematic of the iterative procedure for solving the conjugate heat transfer problem

3 Results and Discussion

The analytical model described in Sec. 2 is validated in a number of different ways. A conjugate heat transfer problem with parameters representative of water cooling of prismatic Li-ion cells discharging at 5C is solved. Based on recently presented data on heat generation rate measurement [46], this C-rate corresponds to 98.5 kW/m^3 heat generation rate. Thermal properties of the Li-ion cell are taken from recent measurements [47]. Specifically, thermal anisotropy is assumed, with the thermal conductivity parallel and normal to the electrode plane assumed to be 30.0 and 0.2 W/m K, respectively. The cell thickness is taken to be 8 mm. The coolant flow speed is assumed to be 0.001 m/s. The ambient temperature is assumed to be 25 °C in all cases considered in this section, so that standard room temperature values for various thermophysical properties of the coolant air are used.

The iterative analytical approach is carried out three separate times assuming three different initial values for the interface temperature. Figure 4 plots the interface temperature as a function of x for all three cases at the end of a number of iterations. Figure 4 shows that for each case, the temperature distribution converges within around 30 iterations and does not change significantly afterward. Based on this, the number of iterations is conservatively taken to be 60 for subsequent investigations in this paper.

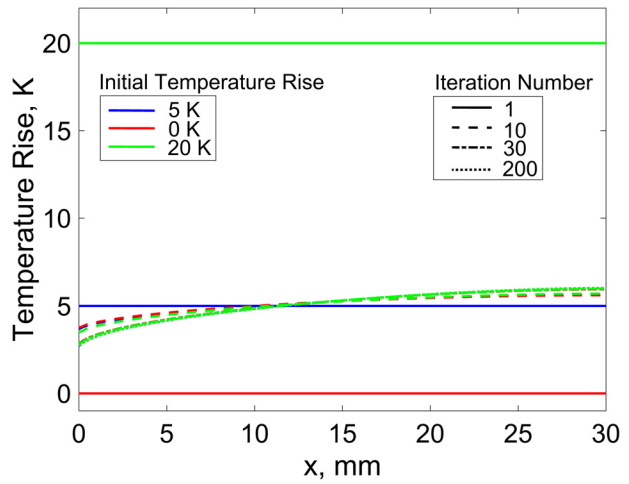

Fig. 4 Plot showing the influence of the initial temperature distribution on the evolution of the solid–fluid interface temperature with number of iterations. This plot shows that in each case, the temperature distribution eventually converges to the same curve.

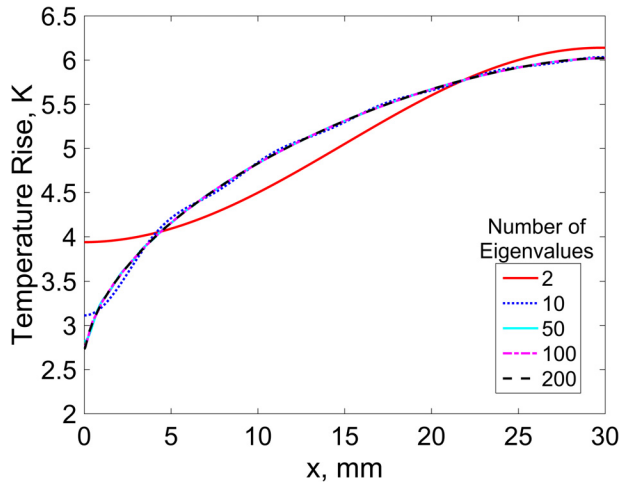

Fig. 5 Plot showing the effect of the number of eigenvalues in the thermal conduction problem on the converged temperature distribution

Figure 4 also shows that the temperature distribution converges to the same curve regardless of the initially assumed temperature distribution. This independence from the initial guess is important and ensures a robust solution even if the initial guess is far from the actual temperature distribution.

While the solution for the thermal conduction equation in the solid body comprises a series summation of infinite terms, this series must in practice be truncated to a finite number of terms. Figure 5 plots the converged temperature distribution at the interface for the problem with the same parameters as Fig. 4 for different numbers of eigenvalues. Figure 5 shows that the temperature solution changes rapidly at low number of eigenvalues, but converges to a stable solution at around 50 eigenvalues. Addition of further eigenvalues does not significantly change the predicted temperature distribution. This is an important observation for reducing computational burden without significant penalty in accuracy. Based on this, a total of 50 eigenvalues are considered in all subsequent figures in this paper.

The iterative technique for determining temperature distribution during Li-ion cell cooling is also validated by comparison with finite element simulations. These simulations utilize the same set of parameters as in the iterative technique. A total of around 500 K elements are used and grid independence is verified. Meshing is refined sufficiently near the leading edge to capture high heat transfer rate and close to the solid-fluid interface to capture boundary layer effects in the fluid domain. The fluid domain is defined to be much larger than expected thickness of velocity and thermal boundary layers. Figure 6(*a*) plots the interface temperature as a function of x for two different C-rates, 4C and 5C, utilizing the same 0.001 m/s water flow for cooling. The heat generation rates at 4C and 5C are 67.8 kW/m^3 and 98.5 kW/m^3, respectively [46]. Plots from both finite element simulations and the analytical model are shown. Figure 6(*a*) shows very good agreement between the two. Further, the heat flux from the solid into the coolant fluid is also plotted as a function of x for finite element simulations and analytical model in Fig. 6(*b*). Similar to the temperature distribution, there is very good agreement for the heat flux distribution. Compared to finite element simulations, the iterative analytical model offers improved computation time, elimination of the need for time-consuming grid generation and a better physical insight into the conjugate problem that governs fluid cooling of a Li-ion cell.

The validated analytical model can be utilized for pack-level thermal design. Specifically, the dependence of thermal performance on various parameters such as geometry, thermophysical properties, etc., can be effectively analyzed. Figure 7(*a*) plots a colormap of the entire cell for a specific case of 5C operation

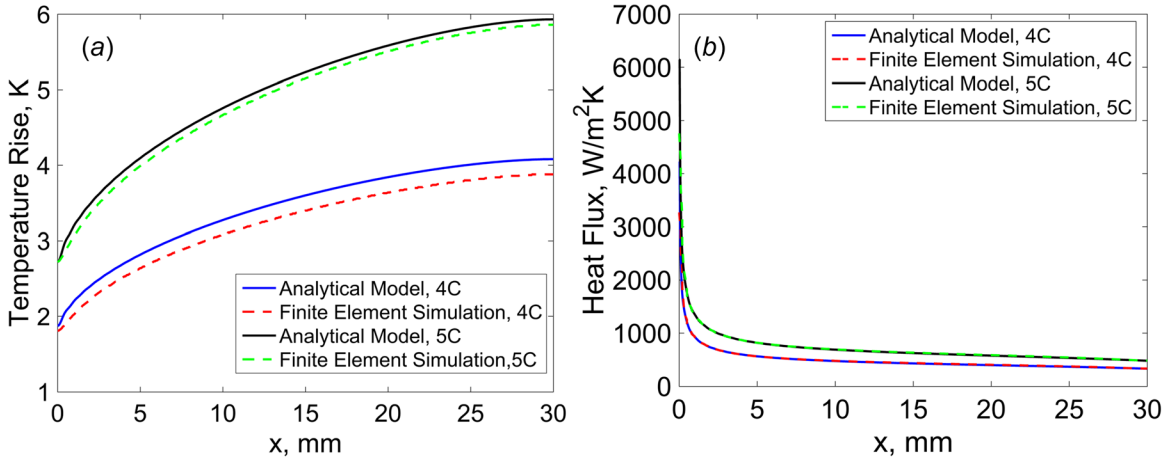

Fig. 6 Comparison of finite element simulation and analytical model for the conjugate heat transfer problem. This comparison is shown for two different C-rates. (*a*) Shows the comparison for interface temperature and (*b*) shows the comparison for interface heat flux.

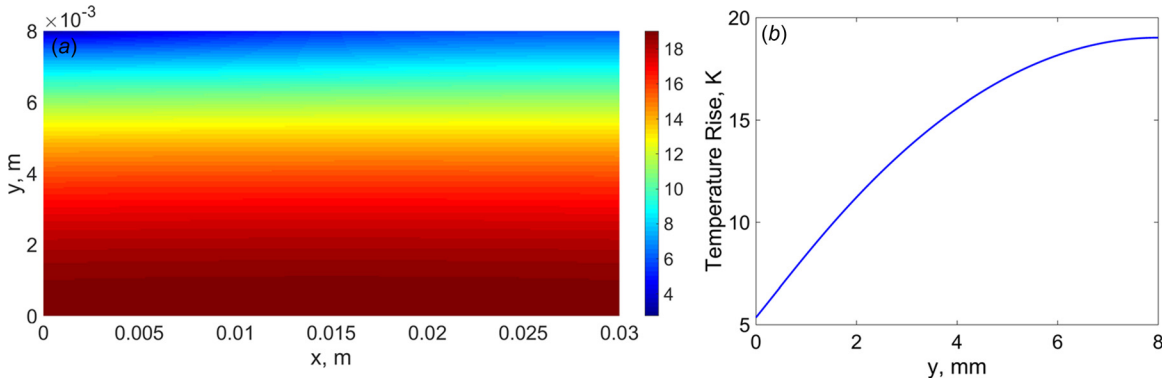

Fig. 7 (*a*) Two-dimensional temperature colormap for a specific set of parameters showing the entire solid cell domain and (*b*) temperature rise as a function of *y* at the center of the cell

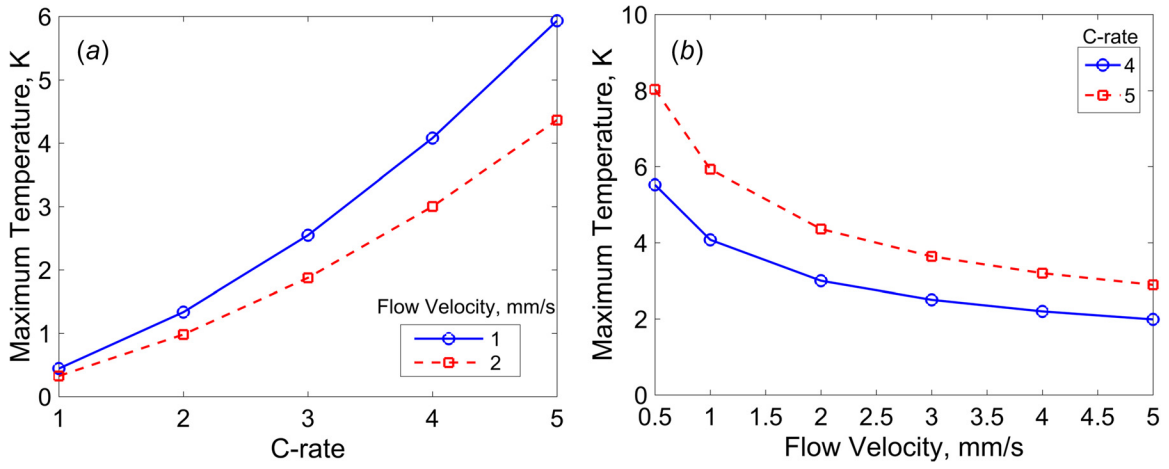

Fig. 8 (*a*) Maximum temperature rise as a function of C-rate for two different coolant fluid flowrates and (*b*) maximum temperature rise as a function of coolant fluid flowrate for two different C-rates

corresponding to 98.5 kW/m^3 while being cooled with 0.001 m/s water flow. The temperature plot shown in Fig. 7(*a*) clearly shows temperature rise within the cell due to heat generation, and the cooling effect of the coolant flow. Figure 7(*b*) further illustrates the temperature field by plotting the temperature rise as a function of y at $x = 15$ mm. Starting from the surface of the cell, the temperature rise increases going inward, and is the highest at the core of the cell, as expected.

A number of other investigations of pack-level thermal management are possible through the iterative analytical model. Figure 8(*a*) plots the peak temperature inside the prismatic cell as a function of C-rate for two different flowrates of water as a coolant. This plot shows a sharp increase in peak temperature rise at the core of the cell with increasing C-rate, which is along expected lines, since the heat generation rate increases quadratically with C-rate [46]. Figure 8(*b*) plots the peak temperature as a

function of flowrate for water as the coolant over a prismatic cell operating at two different C-rates. This plot shows a reduction in peak temperature as the coolant flow increases, but this effect saturates somewhat at higher flowrates. This is an important observation as it shows that merely increasing the coolant flowrate does not necessarily keep improving overall performance, but rather this results in diminishing returns at large flowrates. The reason behind the temperature rise not dropping to insignificant levels at higher flowrates is the nonzero thermal resistance within the cell material which remains constant regardless of the coolant flowrate outside the cell.

It is of interest to compare the performance of various coolant fluids. Figure 9 plots the surface temperature as a function of x for two different C-rates, and compares the performance of water and FC72, a dielectric fluid. Figure 9 shows that for both C-rates, the temperature rise is lower for water compared to FC72, due to superior thermophysical properties of water. A key drawback with water, however, is the potential for electrical damage in case of leakage. Due to its inherently dielectric nature, FC72 does not present this risk, but has somewhat lower thermal performance.

The iterative analytical model can also be used to study the effect of geometry on the thermal performance of the coolant flow. Figure 10 plots the surface temperature of the Li-ion cell as a function of different widths of the Li-ion cell, holding the volumetric heat generation rate constant at 98.5 kW/m^3. Figure 10 shows that at the same C-rate, a thicker cell results in greater temperature rise than a thinner cell. This presents an important design trade-off because a thicker cell will also result in higher pack-level energy storage density, which, while desirable, comes at the cost of increased peak temperature in thicker cells.

Strategies for enhancement of thermal conductivity in Li-ion cells have been proposed in the past [6]. It is of interest to analyze the impact of such cell-level enhancement on pack-level thermal management. An analysis is carried out to determine the required coolant fluid velocity for multiple values of the cell thermal conductivity $k_{y,s}$ in order to maintain the same maximum temperature rise in the cell as a baseline case. A heat generation rate of 98.5 kW/m^3 corresponding to 5C discharge rate is used here. Results presented in Fig. 11 show a significant reduction in the required fluid velocity as $k_{y,s}$ increases from 0.2 W/m K to 0.4 W/m K. However, further increase in thermal conductivity is not found to be as advantageous, because convective heat transfer resistance now begins to dominate over thermal conduction resistance. This analysis shows that increased thermal conductivity of constituting Li-ion cells may positively impact system level coolant flow requirements such as pump work, size of coolant manifold, etc., and ultimately the pack-level energy storage density.

Finally, Fig. 12 analyzes the effect of a non-heat-generating plate inserted between the Li-ion cell and the coolant flow. This could be done in practice to physically separate the heat-

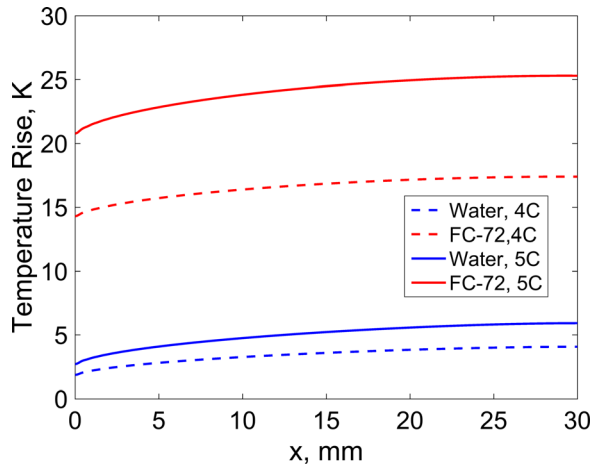

Fig. 9 Interface temperature as a function of *x* for water and FC72 at two different C-rates

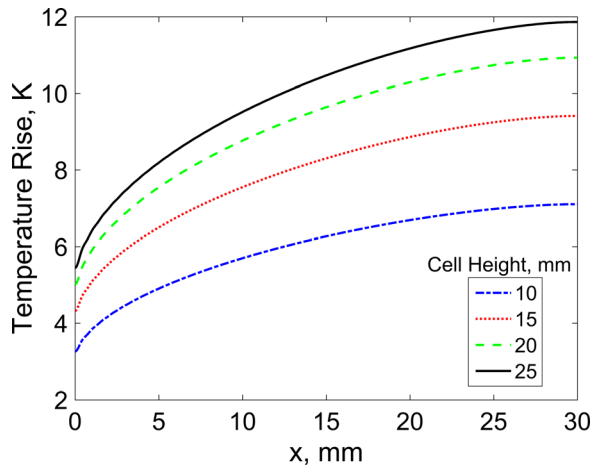

Fig. 10 Interface temperature rise as a function of *x* for different cell thicknesses at 5C discharge rate

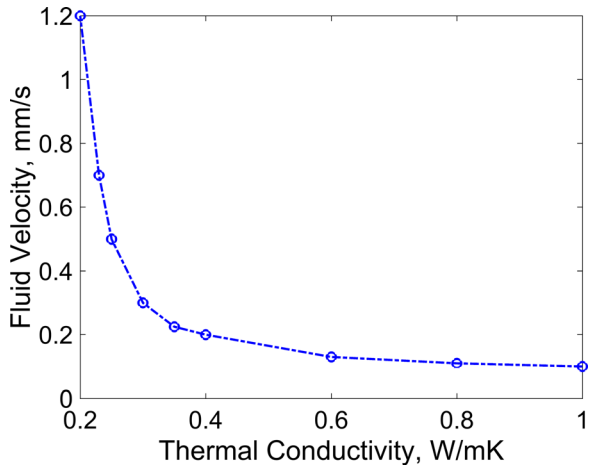

Fig. 11 Coolant flowrate needed to maintain a certain peak cell temperature as a function of the through-plane thermal conductivity k_y of the cell

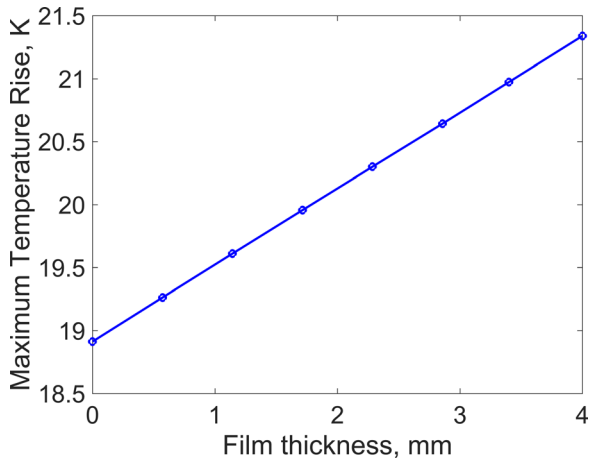

Fig. 12 Peak cell temperature rise as a function of interfacial material thickness at 5C discharge cell cooled by 0.001 m/s water flow

generating cell from the coolant. However, doing so would result in increased temperature rise in the cell due to the additional thermal resistance of the plate. The iterative analytical model can account for this by including an additional, one-dimensional thermal resistance during the process of interfacing the solid and fluid heat transfer models. Figure 12 plots the peak temperature in the cell operating at 5C as a function of the thickness of the interface plate, which is assumed to be made of a plastic material of thermal conductivity of 1.0 W/m K. Figure 12 shows a significant impact of the interface plate on the cell temperature, which worsens with increasing plate thickness. This highlights an important consideration in pack-level thermal management design.

Design trade-offs such as those illustrated above are difficult to analyze using finite element simulation tools due to computational complexity. On the other hand, such trade-offs can be easily analyzed using the iterative analytical method described here, which allows rapid analysis of the impact of various design choices as well as the effect of various geometry parameters and thermophysical properties on the performance of pack-level thermal management.

Note that a significant shortcoming of the analytical model presented here is that it is limited to analysis of steady-state performance. Transient conditions are often relevant for the operation of Li-ion battery pack, in which case, the model presented here must be expanded to account for transient phenomena. In general, deriving transient solutions is not straightforward, particularly for the flow problem in the fluid domain. Nevertheless, the present model provides useful guidelines for designing thermal management systems for Li-ion battery pack, as demonstrated in Figs. 9–12.

4 Conclusions

Heat removal from a Li-ion cell battery pack is critical not only for safety and reliability, but also for optimal performance. Analytical models such as the one presented in this paper may be helpful in analyzing and optimizing the design of pack-level thermal management systems involving the removal of heat generated in cells with a coolant flow. Such models help determine the effect of various parameters on cooling efficiency, and help identify optimal parametric design spaces. Such analytical models are also important for multiphysics co-optimization since several thermal management related parameters also profoundly affect the electrochemical performance of the cell. By developing a robust model for analyzing heat transfer in a fluid-cooled Li-ion battery pack, this paper contributes toward improved thermal and electrochemical performance.

Funding Data

- National Science Foundation (CAREER Award No. CBET-1554183).

Nomenclature

h = convective heat transfer coefficient
H = height
k = thermal conductivity
L = length
Pr = Prandtl number
q'' = heat flux
Q''' = volumetric heat generation rate
Re = Reynolds number
T = temperature
u, v = velocity components
α = thermal diffusivity
β = blend factor

Subscripts

f = fluid
s = solid
x, y = coordinates
0 = interface

References

[1] Scrosati, B., Hassoun, J., and Sun, Y.-K., 2011, "Lithium-Ion Batteries. A Look Into the Future," Energy Environ. Sci., **4**(9), pp. 3287–3295.
[2] Goodenough, J., and Park, K.-S., 2013, "The Li-Lon Rechargeable Battery: A Perspective," J. Am. Chem. Soc., **135**(4), pp. 1167–1176.
[3] Shah, K., Vishwakarma, V., and Jain, A., 2016, "Measurement of Multiscale Thermal Transport Phenomena in Li-Ion Cells: A Review," ASME J. Electrochem. Energy Convers. Storage, **13**(3), p. 030801.
[4] Shah, K., Drake, S. J., Wetz, D. A., Ostanek, J. K., Miller, S. P., Heinzel, J. M., and Jain, A., 2014, "Modeling of Steady-State Convective Cooling of Cylindrical Li-Ion Cells," J. Power Sources, **258**, pp. 374–381.
[5] Shah, K., Drake, S. J., Wetz, D. A., Ostanek, J. K., Miller, S. P., Heinzel, J. M., and Jain, A., 2014, "An Experimentally Validated Transient Thermal Model for Cylindrical Li-Ion Cells," J. Power Sources, **271**, pp. 262–268.
[6] Vishwakarma, V., Waghela, C., Wei, Z., Prasher, R., Nagpure, S. C., Li, J., Liu, F., Daniel, C., and Jain, A., 2015, "Heat Transfer Enhancement in a Lithium-Ion Cell Through Improved Material-Level Thermal Transport," J. Power Sources, **300**, pp. 123–131.
[7] Shah, K., Balsara, N., Banerjee, S., Chintapalli, M., Cocco, A. P., Chiu, W. K. S., Lahiri, I., Martha, S., Mistry, A., Mukherjee, P., Ramadesigan, V., Sharma, C. S., Subramanian, V. R., Mitra, S., and Jain, A., 2017, "State-of-the-Art and Future Research Needs for Multiscale Analysis of Li-Ion Cells," ASME J. Electrochem. Energy Convers. Storage, **14**(2), p. 020801.
[8] Giuliano, M. R., Prasad, A. K., and Advani, S. G., 2012, "Experimental Study of an Air-Cooled Thermal Management System for High Capacity Lithium–Titanate Batteries," J. Power Sources, **216**, pp. 345–352.
[9] Xu, X. M., and He, R., 2013, "Research on the Heat Dissipation Performance of Battery Pack Based on Forced Air Cooling," J. Power Sources, **240**, pp. 33–41.
[10] Yu, K., Yang, X., Cheng, Y., and Li, C., 2014, "Thermal Analysis and Two-Directional Air Flow Thermal Management for Lithium-Ion Battery Pack," J. Power Sources, **270**, pp. 193–200.
[11] Wang, T., Tseng, K. J., Zhao, J., and Wei, Z., 2014, "Thermal Investigation of Lithium-Ion Battery Module With Different Cell Arrangement Structures and Forced Air-Cooling Strategies," Appl. Energy, **134**, pp. 229–238.
[12] Nieto, N., Díaz, L., Gastelurrutia, J., Blanco, F., Ramos, J. C., and Rivas, A., 2014, "Novel Thermal Management System Design Methodology for Power Lithium-Ion Battery," J. Power Sources, **272**, pp. 291–302.
[13] Jin, L. W., Lee, P. S., Kong, X. X., Fan, Y., and Chou, S. K., 2014, "Ultra-Thin Minichannel LCP for EV Battery Thermal Management," Appl. Energy, **113**, pp. 1786–1794.
[14] Huo, Y., Rao, Z., Liu, X., and Zhao, J., 2015, "Investigation of Power Battery Thermal Management by Using Mini-Channel Cold Plate," Energy Convers. Manage., **89**, pp. 387–395.
[15] Hirano, H., Tajima, T., Hasegawa, T., Sekiguchi, T., and Uchino, M., 2014, "Boiling Liquid Battery Cooling for Electric Vehicle," IEEE Conference and Expo on Transportation Electrification Asia-Pacific (ITEC Asia-Pacific), Beijing, China, Aug. 31–Sept. 3, pp. 1–4.
[16] van Gils, R. W., Danilov, D., Notten, P. H. L., Speetjens, M. F. M., and Nijmeijer, H., 2014, "Battery Thermal Management by Boiling Heat-Transfer," Energy Convers. Manage., **79**, pp. 9–17.
[17] Rao, Z., Wang, S., Wu, M., Lin, Z., and Li, F., 2013, "Experimental Investigation on Thermal Management of Electric Vehicle Battery With Heat Pipe," Energy Convers. Manage., **65**, pp. 92–97.
[18] Anthony, D., Wong, D., Wetz, D., and Jain, A., 2017, "Improved Thermal Performance of a Li-Ion Cell Through Heat Pipe Insertion," J. Electrochem. Soc., **164**(6), pp. A961–A967.
[19] Wang, Q., Jiang, B., Xue, Q. F., Sun, H. L., Li, B., Zou, H. M., and Yan, Y. Y., 2015, "Experimental Investigation on EV Battery Cooling and Heating by Heat Pipes," Appl. Therm. Eng., **88**, pp. 54–60.
[20] Tran, T. H., Harmand, S., and Sahut, B., 2014, "Experimental Investigation on Heat Pipe Cooling for Hybrid Electric Vehicle and Electric Vehicle Lithium-Ion Battery," J. Power Sources, **265**, pp. 262–272.
[21] Tran, T. H., Harmand, S., Desmet, B., and Filangi, S., 2014, "Experimental Investigation on the Feasibility of Heat Pipe Cooling for HEV/EV Lithium-Ion Battery," Appl. Therm. Eng., **63**(2), pp. 551–558.
[22] Zhao, R., Gu, J., and Liu, J., 2015, "An Experimental Study of Heat Pipe Thermal Management System With Wet Cooling Method for Lithium Ion Batteries," J. Power Sources, **273**, pp. 1089–1097.
[23] Burban, G., Ayel, V., Alexandre, A., Lagonotte, P., Bertin, Y., and Romestant, C., 2013, "Experimental Investigation of a Pulsating Heat Pipe for Hybrid Vehicle Applications," Appl. Therm. Eng., **50**(1), pp. 94–103.
[24] Goli, P., Legedza, S., Dhar, A., Salgado, R., Renteria, J., and Balandin, A. A., 2014, "Graphene-Enhanced Hybrid Phase Change Materials for Thermal Management of Li-Ion Batteries," J. Power Sources, **248**, pp. 37–43.
[25] Al Hallaj, S., and Selman, J. R., 2000, "A Novel Thermal Management System for Electric Vehicle Batteries Using Phase-Change Material," J. Electrochem. Soc., **147**(9), pp. 3231–3236.
[26] Khateeb, S. A., Amiruddin, S., Farid, M., Selman, J. R., and Al-Hallaj, S., 2005, "Thermal Management of Li-Ion Battery With Phase Change Material for Electric Scooters: Experimental Validation," J. Power Sources, **142**(1), pp. 345–353.

[27] Lin, C., Xu, S., Chang, G., and Liu, J., 2015, "Experiment and Simulation of a $LiFePO_4$ Battery Pack With a Passive Thermal Management System Using Composite Phase Change Material and Graphite Sheets," J. Power Sources, **275**, pp. 742–749.
[28] Babapoor, A., Azizi, M., and Karimi, G., 2015, "Thermal Management of a Li-Ion Battery Using Carbon Fiber-PCM Composites," Appl. Therm. Eng., **82**, pp. 281–290.
[29] Hémery, C. V., Pra, F., Robin, J. F., and Marty, P., 2014, "Experimental Performances of a Battery Thermal Management System Using a Phase Change Material," J. Power Sources, **270**, pp. 349–358.
[30] Ling, Z., Wang, F., Fang, X., Gao, X., and Zhang, Z., 2015, "A Hybrid Thermal Management System for Lithium Ion Batteries Combining Phase Change Materials With Forced-Air Cooling," Appl. Energy, **148**, pp. 403–409.
[31] Park, H., 2013, "A Design of Air Flow Configuration for Cooling Lithium Ion Battery in Hybrid Electric Vehicles," J. Power Sources, **239**, pp. 30–36.
[32] Fathabadi, H., 2014, "A Novel Design Including Cooling Media for Lithium-Ion Batteries Pack Used in Hybrid and Electric Vehicles," J. Power Sources, **245**, pp. 495–500.
[33] Fan, L., Khodadadi, J. M., and Pesaran, A. A., 2013, "A Parametric Study on Thermal Management of an Air-Cooled Lithium-Ion Battery Module for Plug-In Hybrid Electric Vehicles," J. Power Sources, **238**, pp. 301–312.
[34] Yang, N., Zhang, X., Li, G., and Hua, D., 2015, "Assessment of the Forced Air-Cooling Performance for Cylindrical Lithium-Ion Battery Packs: A Comparative Analysis Between Aligned and Staggered Cell Arrangements," Appl. Therm. Eng., **80**, pp. 55–65.
[35] Mahamud, R., and Park, C., 2011, "Reciprocating Air Flow for Li-Ion Battery Thermal Management to Improve Temperature Uniformity," J. Power Sources, **196**(13), pp. 5685–5696.
[36] Wu, M. S., Liu, K. H., Wang, Y. Y., and Wan, C. C., 2002, "Heat Dissipation Design for Lithium-Ion Batteries," J. Power Sources, **109**(1), pp. 160–166.
[37] Karimi, G., and Dehghan, A. R., 2012, "Thermal Management Analysis of a Lithium-Ion Battery Pack Using Flow Network Approach," Int. J. Mech. Eng. Mechatronics, **1**(1), pp. 88–94.
[38] Tong, W., Somasundaram, K., Birgersson, E., Mujumdar, A. S., and Yap, C., 2015, "Numerical Investigation of Water Cooling for a Lithium-Ion Bipolar Battery Pack," Int. J. Therm. Sci., **94**, pp. 259–269.
[39] Jarrett, A., and Kim, I. Y., 2011, "Design Optimization of Electric Vehicle Battery Cooling Plates for Thermal Performance," J. Power Sources, **196**(23), pp. 10359–10368.
[40] Jarrett, A., and Kim, I. Y., 2014, "Influence of Operating Conditions on the Optimum Design of Electric Vehicle Battery Cooling Plates," J. Power Sources, **245**, pp. 644–655.
[41] Khateeb, S. A., Farid, M. M., Selman, J. R., and Al-Hallaj, S., 2004, "Design and Simulation of a Lithium-Ion Battery With a Phase Change Material Thermal Management System for an Electric Scooter," J. Power Sources, **128**(2), pp. 292–307.
[42] Mills, A., and Al-Hallaj, S., 2005, "Simulation of Passive Thermal Management System for Lithium-Ion Battery Packs," J. Power Sources, **141**(2), pp. 307–315.
[43] Shah, K., and Jain, A., 2015, "An Iterative, Analytical Method for Solving Conjugate Heat Transfer Problems," Int. J. Heat Mass Transfer, **90**, pp. 1232–1240.
[44] Kays, W. M., and Crawford, M. E., 1993, *Convective Heat and Mass Transfer*, McGraw-Hill, New York.
[45] Hahn, D. W., and Özişik, M. N., 2012, *Heat Conduction*, 3rd ed., Wiley, Hoboken, NJ.
[46] Drake, S. J., Martin, M., Wetz, D. A., Ostanek, J. K., Miller, S. P., Heinzel, J. M., and Jain, A., 2015, "Heat Generation Rate Measurement in a Li-Ion Cell at Large C-Rates Through Temperature and Heat Flux Measurements," J. Power Sources, **285**, pp. 266–273.
[47] Drake, S. J., Wetz, D. A., Ostanek, J. K., Miller, S. P., Heinzel, J. M., and Jain, A., 2014, "Measurement of Anisotropic Thermophysical Properties of Cylindrical Li-Ion Cells," J. Power Sources, **252**, pp. 298–304.